

Influence of processing techniques on the properties of YAG:Ce nanophosphor

Kai Zhang, Wenbin Hu, Yating Wu, Hezhou Liu *

State Key Laboratory of Metal Matrix Composites, Shanghai Jiao Tong University, Shanghai 200240, China

Received 11 June 2007; received in revised form 11 November 2007; accepted 6 February 2008

Available online 4 June 2008

Abstract

Influence of three post treatment techniques including water washing, ethanol washing and *n*-butanol heterogeneous azeotropic distillation on the structure, dispersity and luminescence properties of YAG:Ce nanophosphor were comparatively studied. In contrast to the first two processing techniques, *n*-butanol azeotropic distillation prevents powders from conglomeration due to larger *n*-butanol molecules, longer butoxy groups and a more complete replacement of residual water in the precipitate. The phosphor from azeotropic distillation exhibits excellent luminescence properties with higher emission intensity than those from water washing and ethanol washing.

© 2008 Elsevier Ltd and Techna Group S.r.l. All rights reserved.

Keywords: A. Powders: chemical preparation; B. Spectroscopy; C. Optical properties

1. Introduction

Recently, a new type of light emitting diodes (LEDs) based on gallium nitride (GaN) that emits blue light has been developed. Trivalent cerium activated yttrium aluminum garnet (YAG:Ce) phosphor has been found to be suitable for converting this blue LEDs radiation into a very broad band yellow emission [1]. The yellow emission complements the blue light to produce white light. Compared with traditional lighting, it has the advantages of high energy-efficiency, high reliability, long life, fast response and non-polluting production.

The current interest in nano-sized phosphor is due to their novel properties such as low calcination temperature, high luminous efficiency, quantum effect, etc. [2–4]. Co-precipitation method is a low-cost and easy method to fabricate nano-sized powders compared with other processes (such as sol–gel, chemical or physical vapor deposition). However, the process suffers from the disadvantage of producing hard agglomerates during drying and calcination procedures [5], which deteriorates the properties of prepared powders [6]. The key issue to decrease agglomeration has been considered to decrease the surface

tension and to overcome hydrogen bonding by replacing water with an organic solvent, since water has a very high surface tension and is bound by strong hydrogen bonds [7]. Surface treatment of gels by organic polymer surfactants has also been used to lower the degree of agglomeration [8]. Recently, a new processing method, heterogeneous azeotropic distillation (HAD), that is free of hard agglomeration, is used to prepare nano-sized powders [9–12].

In this research, YAG:Ce nanophosphor was synthesized without agglomerates, using also the HAD technique. Two regular processing techniques, water washing and ethanol washing were also comparatively studied.

2. Materials and experimental procedures

2.1. Materials

The original materials for YAG:Ce phosphor were rare earth oxide Y_2O_3 (99.99%), $Ce(NO_3)_3 \cdot 6H_2O$ (A.R.) and $Al(NO_3)_3 \cdot 9H_2O$ (A.R.).

Y_2O_3 was dissolved in dilute HNO_3 . $Ce(NO_3)_3 \cdot 6H_2O$ and $Al(NO_3)_3 \cdot 9H_2O$ were dissolved in deionized water. The multi-cation solution was prepared according to stoichiometric proportion of $Y_{2.95}Ce_{0.05}Al_{5.0}O_{12}$. Ammonium hydrogen carbonate was selected as precipitant.

* Corresponding author. Tel.: +86 21 62933585; fax: +86 21 62822012.

E-mail address: jh13zhang@hotmail.com (H. Liu).

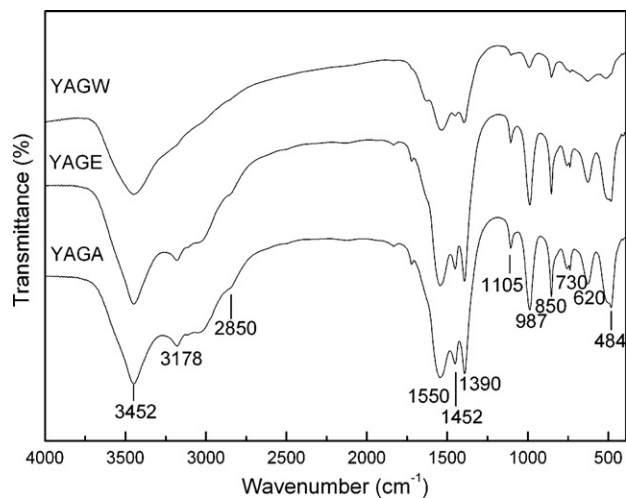


Fig. 1. FT-IR spectra of YAGW, YAGE and YAGA.

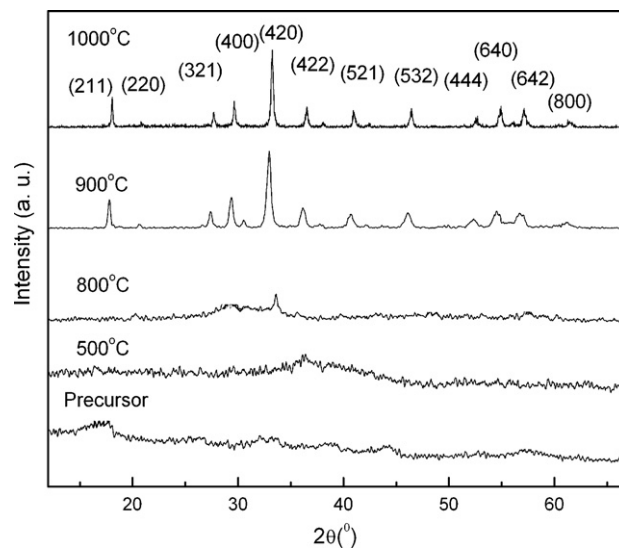


Fig. 2. XRD patterns of the precursor calcined at different temperature.

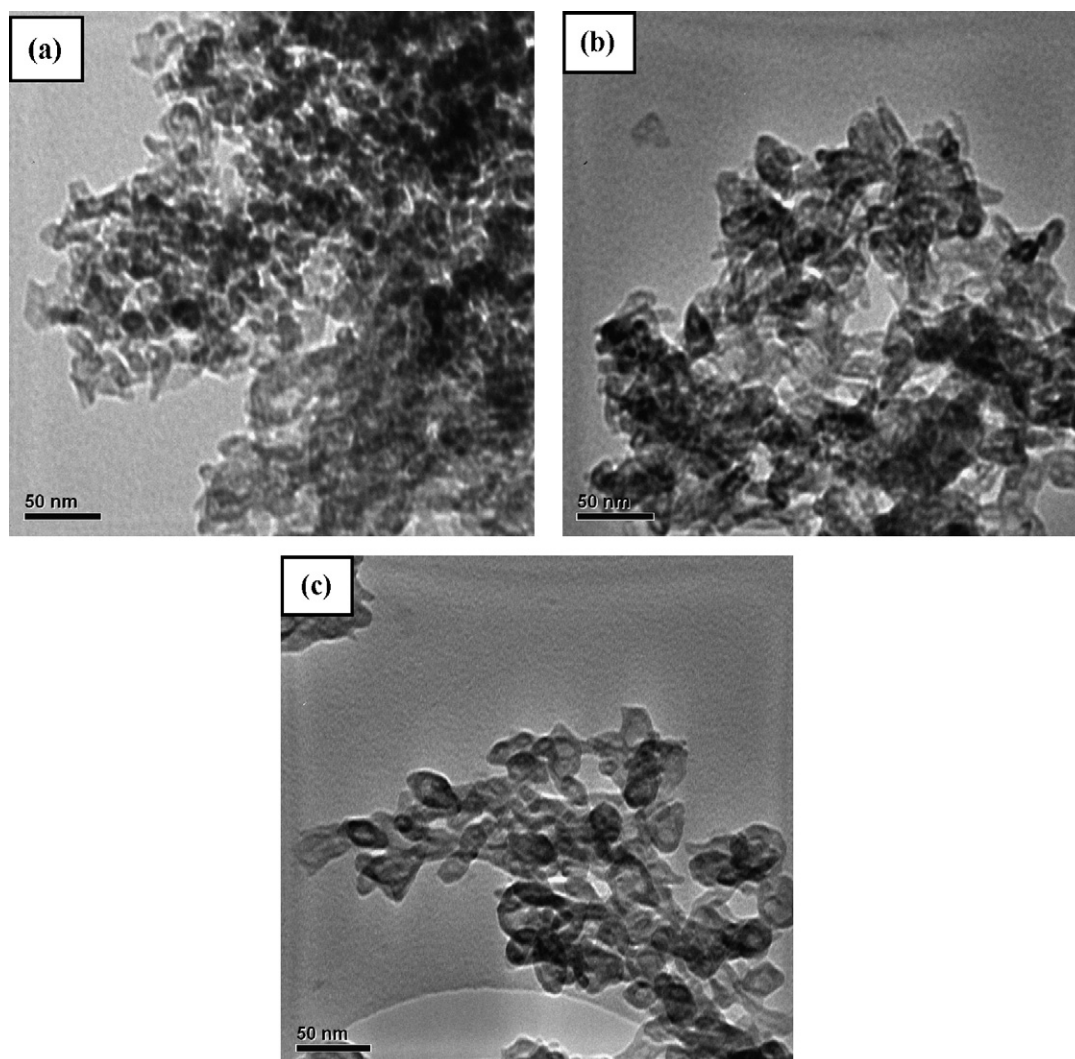


Fig. 3. TEM images of (a) YAGW, (b) YAGE and (c) YAGA.

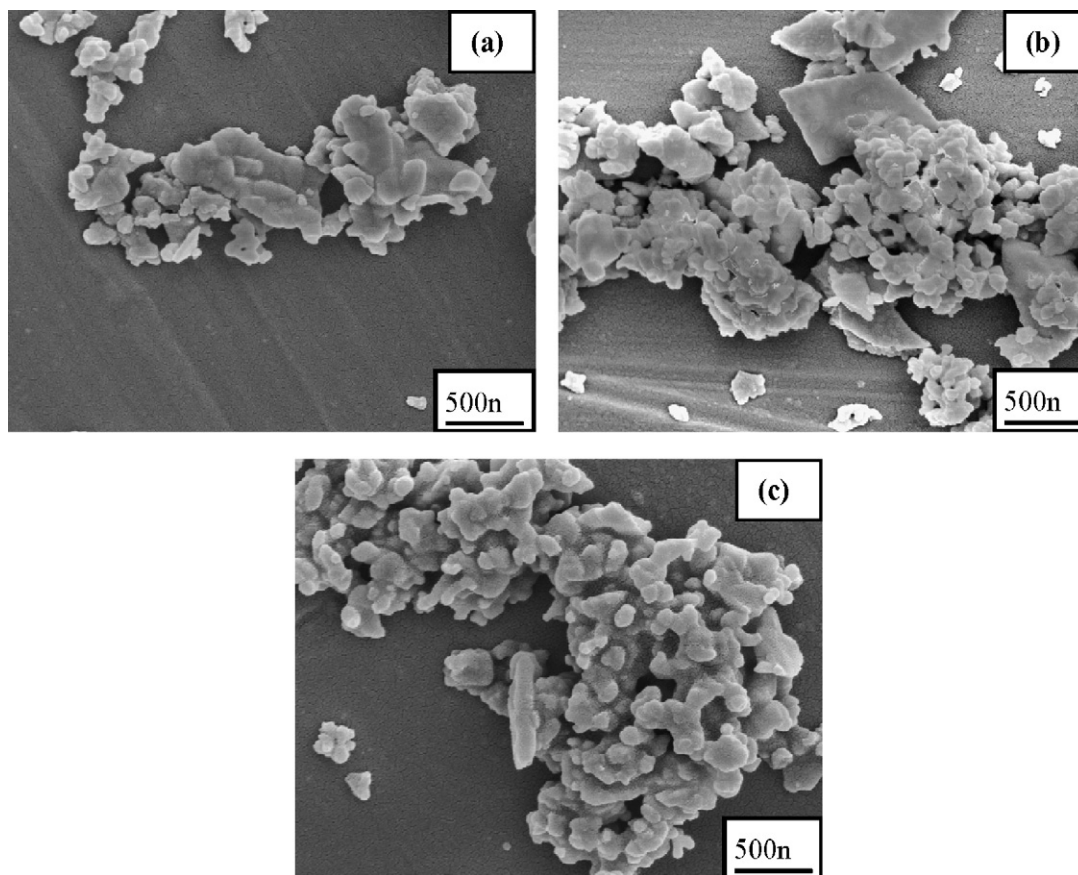


Fig. 4. SEM images of (a) CYAGW, (b) CYAGE and (c) CYAGA.

2.2. Powder synthesis

Precursors were produced by dropping multi-cation solution into the precipitant solution under magnetic stirring at room temperature. It was stirred another 30 min after dropping. Resultant suspensions, after aging for 8 h at 50 °C, were filtered, washed with deionized water until the filter cake became neutral to pH paper. The cake was divided into three parts. One part was dried at 120 °C over 12 h and then ground by agate mortar (sample YAGW). The second part was washed with ethanol and dried at 120 °C over 12 h (sample YAGE). The third part was completely dispersed with *n*-butanol and HAD treated. Water in the mixture was removed when the temperature reached 93 °C. Then the azeotropic system was refluxed at 117 °C (the boiling point of *n*-butanol) for 1 h. After cooling, the precursors were recovered and dried at 120 °C over 12 h (sample YAGA). The samples YAGW, YAGE and YAGA were calcined at 1200 °C for 3 h in a gas mixture of nitrogen and 8% (v/v) of hydrogen. The corresponding calcination products were denoted CYAGW, CYAGE and CYAGA, respectively.

2.3. Powder characterization

Fourier transform infrared spectra (FT-IR) were recorded by Equinox Fourier transform infrared spectrometer. X-ray

diffraction (XRD) was carried out on a Rigaku D/Max X-ray diffractometer with Cu K α radiation and scanning speed of 3° min⁻¹. Powder morphology and dispersity were observed using a transmission electron microscope (TEM; JEM-2010) and a field emission scanning electron microscopy (FESEM; FEI SIRION 200). Size distributions were estimated by using of photon correlation spectroscopy particle size analyzer (Zetasizer Nano S). Excitation and emission spectra were obtained on a LS 50B luminescence spectrometer at room temperature.

3. Results and discussion

3.1. Surface modification during post treatment

The FT-IR spectra of as-dried samples are shown in Fig. 1. The peak around 3452 cm⁻¹ corresponded to OH⁻ group. Other peaks at about 3178, 1550, 1390 and 987 cm⁻¹ were attributed to NH₄⁺ and NO₃⁻ vibrations, respectively. The peaks at about 620 and 484 cm⁻¹ represented the characteristics Al–O metal–oxygen vibrations, while the peak at 730 cm⁻¹ represented the Y–O vibration [13]. The peaks around 1452 and 1105 cm⁻¹ were assigned to C–O vibrations. The difference between YAGA or YAGE and YAGW can be seen from the C–H stretching vibration near 2850 cm⁻¹. These results illustrated some *n*-butanol or ethanol molecules chemisorbed on the surface of the YAGA or YAGE particles.

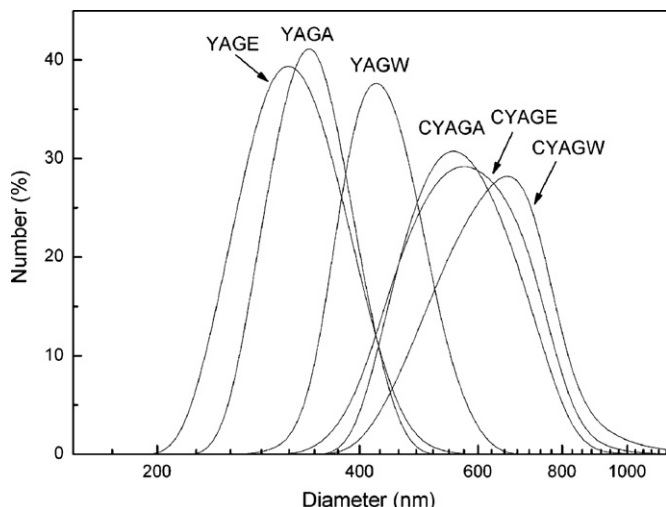


Fig. 5. Particle size distributions of powders.

3.2. Phase transition during calcination

Because the phase development of YAGW, YAGE and YAGA was identical, only the XRD patterns of YAGW at different calcination temperature from 500 to 1000 °C are given in Fig. 2.

The powders were found to be amorphous below 800 °C. The powders started to crystallize as pure YAG at 900 °C. The intermediate phases like YAP and YAM, which do not favor luminescence, are completely eliminated. Co-precipitation method mixes materials at molecular level. Therefore, the precursor had a high homogeneity and reactivity, which induced lower calcination temperature.

3.3. Powder morphology

Typical TEM images of precursors treated by three techniques and SEM images of their corresponding calcined powders are shown in Figs. 3 and 4, respectively. YAGW particles from water washing presented compact agglomerates. Contrast, YAGA, i.e. particles treated by AHD were well dispersive. After calcination, particles merged and grew. Partial CYAGW particles came into a micrometer dimension, while mostly CYAGA particles maintained the nanometer size.

Fig. 5 shows size distributions of YAGW, YAGE, YAGA and their calcined powders. The size distribution of YAGA was much narrower than YAGW and YAGE. After calcination, all size distributions broadened. The dispersity of CYAGA was much better than CYAGW and CYAGE.

3.4. Luminescence properties

The ground state of Ce is 4f. The ground state of Ce is split into $^2F_{5/2}$ and $^2F_{7/2}$ with an energy difference of about 2200 cm^{-1} , due to spin–orbit coupling. The next excited state is 5d. The 4f–5d transitions are parity and spin allowed. In the YAG host crystal, Ce occupies the site of the strong crystal field of O^{2-} . The 5d is split by the crystal field [14,15] and hence there are more than one absorption band in the excitation

spectrum in the region between 200 and 500 nm. Among them, the excitation band covering 400–500 nm is the most intense band. In the emission spectrum, the band located between 500 and 700 nm is a yellow light.

Fig. 6 shows the luminescence properties of phosphors with different treatment. Different processing techniques did not affect the location of excitation and emission bands. The excitation band was about 460 nm. The emission band was around 520 nm. The emission intensity of phosphors changed as $I(\text{CYAGA}) > I(\text{CYAGE}) > I(\text{CYAGW})$, which indicated HAD treatment is an effective method to improve luminescence properties of precipitation prepared nanophosphor.

Hard agglomeration occurs upon drying and calcination due to hydrogen bonding. After calcination, the hydrogen bonding among particles may form non-radiative centers. The high face tension of particles increased the possibility of surface defect traps formation. By introducing HAD or ethanol washing, residual water in the precipitate was substituted by *n*-butanol or ethanol with a lower surface tension and the surface OH^- groups were replaced by $n\text{-CH}_3(\text{CH}_2)_3\text{O}^-$ groups or by $\text{C}_2\text{H}_5\text{O}^-$ groups. As a result, strong hydrogen bonding was

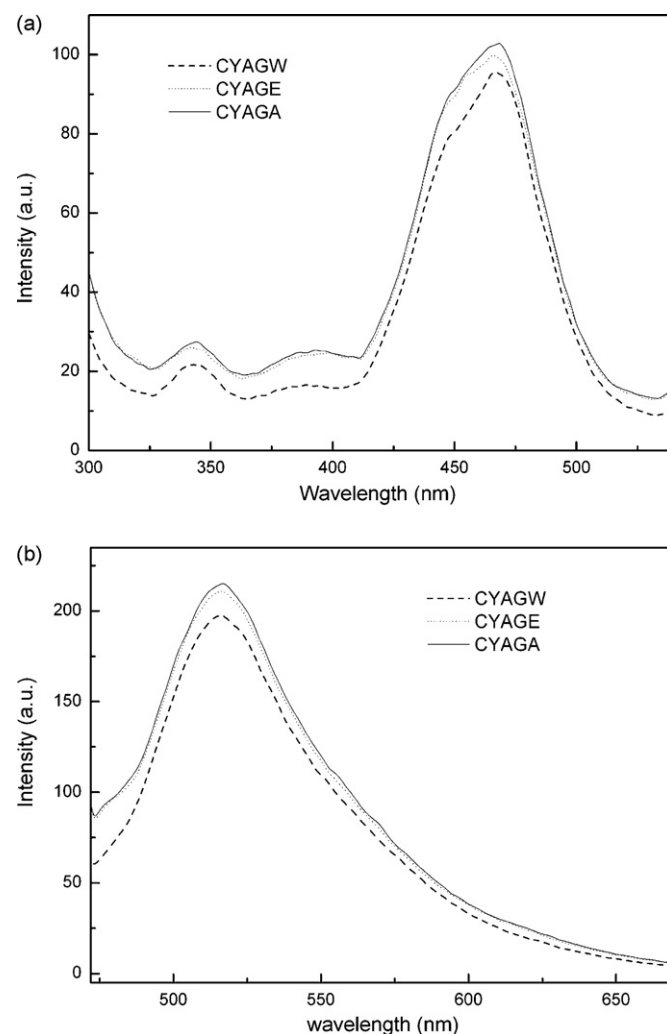


Fig. 6. Excitation (a, $\lambda_{\text{em}} = 560\text{ nm}$) and emission (b, $\lambda_{\text{ex}} = 460\text{ nm}$) spectra of phosphors.

eliminated. The probability of formation of non-radiative centers reduced. HAD technique was more effective than ethanol washing. Therefore, emission intensity of CYAGA was stronger than CYAGE and CYAGW.

4. Conclusions

YAG:Ce precursors were prepared through three processing techniques including water washing, ethanol washing and *n*-butanol heterogeneous azeotropic distillation. Ethanol washing and heterogeneous azeotropic distillation replaced water molecules by $\text{C}_2\text{H}_5\text{O}^-$ groups or $n\text{-CH}_3(\text{CH}_2)_3\text{O}^-$ groups, which absorbed on the surface of precursors. These chemical replacements can prevent conglomeration by decreasing surface tension and eliminating hydrogen bonds among adjacent hydrated particles. Because of a more complete substitution of water, the precursor from *n*-butanol heterogeneous azeotropic distillation has been much more dispersive. Complete substitution of water resulted here in decreasing the possibility of formation of non-radiative centers. Therefore, luminescent intensity of phosphor from azeotropic distillation was stronger than those from ethanol washing and water washing.

Acknowledgement

The authors would like to thank Instrumental Analysis Center of Shanghai Jiao Tong University for sample characterization.

References

- [1] Y. Pan, M. Wu, Q. Su, Comparative investigation on synthesis and photoluminescence of YAG:Ce phosphor, *Mater. Sci. Eng. B* 106 (2004) 251–256.
- [2] D. Haranath, H. Chande, P. Shama, S. Sigh, Enhanced luminescence of $\text{Y}_3\text{Al}_5\text{O}_{12}:\text{Ce}^{3+}$ nanophosphor for white light emitting diodes, *Appl. Phys. Lett.* 89 (2006) 1731181–1731183.
- [3] L. Zhou, B. Yan, In situ synthesis and optical properties of strong red emitting nanomaterial: $\text{Y}_x\text{Gd}_{2-x}\text{O}_3:\text{Eu}^{3+}$ by composing different hybrid polymeric precursors, *Ceram. Int.* 32 (2) (2006) 207–211.
- [4] J. Zhang, H. Feng, W. Hao, T. Wang, Luminescence of nanosized ZnO/polyaniline films prepared by self-assembly, *Ceram. Int.* 33 (5) (2007) 785–788.
- [5] J. Li, T. Ikegami, J. Lee, M. Toshiyuki, Y. Yoshiyuk, Co-precipitation synthesis and sintering of yttrium aluminum garnet (YAG) powders: the effect of precipitant, *J. Eur. Ceram. Soc.* 20 (2000) 2395–2405.
- [6] K. Song, J. Kim, Synthesis of high surface area tin oxide powders via water-in-oil micro emulsions, *Powder Technol.* 107 (3) (2000) 268–272.
- [7] T. Okubo, H. Nagamoto, Low-temperature preparation of nanostructured zirconia and YSZ by sol–gel processing, *J. Mater. Sci.* 30 (1995) 749–757.
- [8] G. Xu, X. Zhang, W. He, H. Liu, H. Li, The study of surfactant application on synthesis of YAG nano-sized powders, *Powder Technol.* 163 (2006) 202–205.
- [9] H. Qu, L. Gao, C. Feng, J. Guo, D. Yang, Preparation of nanoscale zirconia powder by heterogeneous azeotropic distillation processing, *J. Inorg. Mater.* 9 (3) (1994) 365–370.
- [10] S.K. Tadokoro, E. Muccillo, Physical characteristics and sintering behavior of ultrafine zirconia-ceria powders, *J. Eur. Ceram. Soc.* 22 (9–10) (2002) 1723–1728.
- [11] B. Li, Y. Zhang, Y. Zhao, Z. Wu, Z. Zhang, A novel method for preparing surface-modified $\text{Mg}(\text{OH})_2$ nanocrystallines, *Mater. Sci. Eng. A* 452–453 (2007) 302–305.
- [12] W. Cai, H. Li, Y. Zhang, Influences of processing techniques of the H_2O_2 -precipitated pseudoboehmite on the structural and textural properties of $\gamma\text{-Al}_2\text{O}_3$, *Colloids Surf. A* 295 (1–3) (2007) 185–192.
- [13] Y. Zhou, J. Li, M. Yu, S. Wang, H. Zhang, Synthesis-dependent luminescence properties of $\text{Y}_3\text{Al}_5\text{O}_{12}:\text{Re}^{3+}$ (Re = Ce, Sm, Tb) phosphors, *Mater. Lett.* 56 (2002) 628–636.
- [14] G. Blasse, A. Bril, A new phosphor for flying-spot cathode-ray tubes for color television: yellow-emitting $\text{Y}_3\text{Al}_5\text{O}_{12}:\text{Ce}^{3+}$, *Appl. Phys. Lett.* 11 (1967) 53–55.
- [15] E. Zych, C. Brecher, J. Glodo, Kinetics of cerium emission in a YAG:Ce single crystal: the role of traps, *J. Phys. Condens. Matter* 12 (2000) 1947–1958.